Impact of Sympathetic Activation in Imaging Photoplethysmography

Vincent Fleischhauer[1] Alexander Woyczyk[1] Stefan Rasche[2]
Sebastian Zaunseder[1]
[1] University of Applied Sciences and Arts Dortmund
Dortmund, Germany
[2] University Hospital Leipzig, Leipzig, Germany
vincent.fleischhauer@fh-dortmund.de

Abstract

Photplethysmography (PPG) is known to reflect changes in sympathetic tone. This contribution investigates the behaviour of imaging photoplethysmography (iPPG) upon sympathetic activation. To that end, we assessed the impact of a distal painful stimulus on the facial iPPG and contralateral finger PPG waveforms. Our results show that alternating components of both signals behave differently. As expected, the alternating component of the finger PPG signal shows a significant and persistent decrease upon stimulus ($p < 0.001$). The alternating component of the iPPG signal shows only a slight decrease followed by a fast increase ($p < 0.01$). The found behaviour might be explained by different degrees of sympathetic responsiveness in the extremities and in the face. Sympathetic activation increases cardiac output and triggers general vasoconstriction. Extremities show highly pronounced vasoconstriction which decreases the alternating component. The facial vasoconstriction is comparatively small. As a result, local vasoconstriction might cause a short-term decrease followed by the contrary effect, namely an increase in the alternating component, driven by an increased systemic pulse pressure. Our finding has relevance for the interpretation of iPPG signals and the design of future use cases beyond remote heart rate assessment. In particular, care should be taken when expectations on the finger PPG are to be transferred to iPPG.

1. Introduction

Photoplethysmography (PPG) captures blood volume changes in the microvascular bed of tissue. The technique provides a non-invasive mean to determine the arterial oxygen saturation (pulse oximetry), which makes it clinically indispensable [1]. Even beyond the arterial oxygen saturation PPG signals hold valuable information as the photoplethysmographic waveform reflects the cardiac ejection and the vascular state [16, 17]. Various works have related the PPG waveform, *i.e*. its amplitude, area, *etc*., and its variations, respectively, to the vasculature in general (vascular age) [3, 4, 6, 11, 25], to dynamic cardiovascular parameters (*e.g*. cardiac output [2, 29] and blood pressure [29]) and to the activity of the autonomous nervous system (ANS) (*e.g*. sympathetic activation upon cold stress [5, 12, 20]).

Over the last years, imaging PPG (iPPG) has gained immense attention. As in conventional PPG, iPPG exploits blood volume changes to derive a pulsatile signal. Instead of a sensor attached to the skin, iPPG works at a distance and uses a camera as sensor [10]. Most works on the iPPG focus on the extraction of the heart rate (HR) and heart rate variability (HRV), respectively [9, 22, 30, 32]. As iPPG recordings are most often heavily distorted by motion and variations in the illumination, HR extraction is a demanding task. However, similar to the conventional PPG waveform, the iPPG waveform can be assumed to feature more information. Only few works have addressed morphological analysis so far *e.g*. [14, 19, 26, 27].

This work investigates the behaviour of the iPPG upon autonomous stimulation. Using the conventional (finger) PPG, a couple of works have shown the alternating component (AC) to decrease upon painful stimulation as a result of increased sympathetic tone [2, 5, 12, 20]. We aim to analyze if a similar reaction in the AC can be revealed from iPPG.

The remainder of the work is structured as follows. Section 2 introduces the used data and applied methods, which cover the general processing of iPPG signals as well as the applied statistics. Section 3 presents the results on the experimental data. Section 4 discusses the results and relates them to works from the literature. Finally, in section 5 we

give an outlook for future works.

2. Methods and Materials

2.1. Data

The data originates from a cold pressure test (CPT). The CPT is a test that provokes pain and thus a physiological response driven by sympathetic activation [24]. During CPT participants immersed one hand into cold water (constant temperature of 3 °C). We recorded the face of the subjects using a RGB camera (UI-3370CP-C-HQ; IDS, Germany) and a near-infrared (NIR) camera (UI-3370CP-NIR-GL; IDS, Germany). Both cameras had a color depth of 12 bit, a frame rate of 100 fps and a resolution of 420×320 pixels. The experimental setup was illuminated by ambient light, a fluorescent ceiling light and a custom NIR illumination. As reference, we recorded the non-invasive continuous blood pressure (Finometer Midi, Finapres Medical Systems), electrocardiogram, finger photoplethysmogram contralateral to the CPT and respiration by a thoracic belt (all sensors from ADInstruments). The captured data was synchronized via ADInstruments' PowerLab. [31] gives a comprehensive overview on the data and experimental procedure.

Before executing the CPT, participants run through a baseline of approx. 480 s. Within the baseline, we defined three analysis intervals (Baseline_1, Baseline_2 and Baseline_3), each one lasting 10 s. The baseline intervals were placed three, two and one minute before the CPT. The CPT lasted up to three minutes. The participants were free to terminate the CPT earlier. In this work we consider two analysis intervals during the CPT: (1) the time interval 10 s after immersion of the hand (denoted as AfterCPT, intended to capture an immediate reaction) and (2) the time interval 5 s before and after the time instant at which the systolic blood pressure reached its peak value (denoted as HighestSBP, regarded as moment of highest sympathetic outflow).

22 healthy subjects (age 25.5 ± 3.73 years, 10 female) participated in the study twice, one time in supine position and one time in sitting position. In consequence of varying recording positions and their temporal separation, different recordings of the same subject were considered independent. One recording had to be discarded due to technical problems, thus 43 recordings remained. Additional recordings were excluded by further processing steps mainly due to subjects' movements. Details on the further exclusion are given in section 2.3. The study has been approved by the institutional review board of TU Dresden (EK119032016). All participants were informed about the experimental procedure and gave written consent.

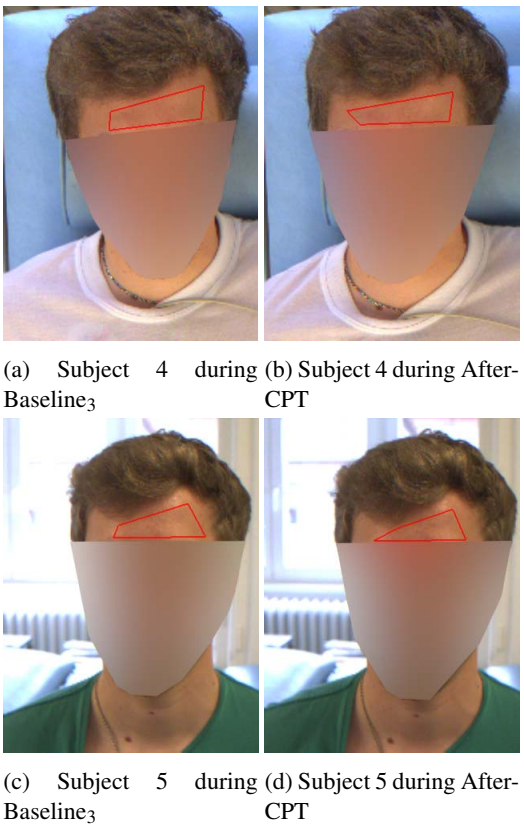

(a) Subject 4 during Baseline_3 (b) Subject 4 during AfterCPT

(c) Subject 5 during Baseline_3 (d) Subject 5 during AfterCPT

Figure 1: Exemplary ROI definitions. The ROI is enclosed by a red line.

2.2. Signal processing

The analysis was done in a semiautomated way in order to diminish the impact of faulty segmentations or wrong beat detections. We focused on the green channel of the video recordings as it provides the highest signal quality [28] (in the discussion we will qualitatively evaluate the NIR channel as well; it was processed equally to the green channel). The applied processing comprised a preprocessing stage to yield time varying signals and a feature extraction stage to acquire the AC.

Preprocessing: For each analysis interval we manually defined a region of interest (ROI) that comprised the forehead of the participant (for examples see figure 1). We then averaged all pixels in the ROI to obtain a pixel trace and inverted it to resemble the conventional PPG. The pixel trace was processed by a bandpass filter with a passband between 0.2 Hz and 8 Hz (by applying two 5th order Butterworth filters of cutoff frequency 8 Hz and cutoff frequency 0.2 Hz, respectively, in forward and backward direction and subtracting their outputs to yield the filtered iPPG signal). The reference PPG was processed in the same way (see figure 3).

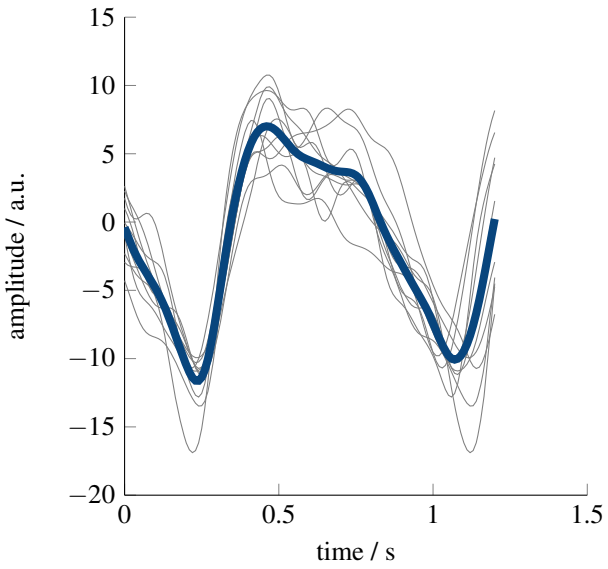

Figure 2: Exemplary template generation. The filtered iPPG signal from figure 3 served as input. Single beat segments are shown in light gray. The resulting template is shown in bold dark blue.

Feature extraction: The feature extraction based on a beat template generated for each of the 10 s analysis intervals. We used the algorithm of Lazaro [15] to detect single pulses using the reference PPG. The used detector places the fiducial point on the rising edge of pulse. We manually checked that there were no relevant phase shifts between the reference PPG and iPPG signal. Around each beat detection t_i we defined a beat segment according to

$$\begin{aligned} start &= t_i - 0.45 \cdot \widetilde{PP} \\ end &= t_i + \widetilde{PP} \end{aligned} \tag{1}$$

where $\widetilde{PP}$ denotes the median interval of all beat-to-beat intervals in the respective analysis interval. Single beat segments were discarded if *start* or *end* according to equation (1) were found to be outside the analysis interval. The remaining beat segments were pairwise correlated. We discarded beat segments that showed a mean correlation to all segments lower than 0.3. From the remaining beat segments we calculated a beat template by ensemble averaging (see figure 2). For analysis intervals that had fewer than three valid beats, no template was calculated. In the template we searched for the first minimum before the detection point, *i.e.* t_i (respectively maximum after the detection point). The amplitude difference between maximum and minimum was defined as AC (ensembleAC) and further analyzed.

2.3. Exclusion Criteria and Statistical Assessment

As stated before, our analysis directs at the AC of the iPPG and reference PPG, respectively. To enhance interpretation, we additionally analyzed the median length of the beat-to-beat intervals (denoted as BBI and derived from the reference PPG signal) and the pulse pressure, thus leading to overall four response variables.

Exclusion criteria: As our analysis directs at exploring physiological mechanism rather than providing an automated processing procedure, we excluded a couple of records because they were likely to corrupt the results. We employed the following exclusion criteria: (1) CPT was terminated early (we required at least 25 s) so that the placement of analysis intervals failed or no stable forehead region could be defined for strong subject movements (four subjects). (2) Template generation failed due to too few beats in the iPPG signal or in the reference PPG (ten subjects). (3) Strong displacements of the subjects' heads between analysis intervals[1] (19 subjects). (4) ROI contained less than 1000 pixels (1 subject) [2] Finally, 24 recordings remained for statistical analysis.

Statistical analysis: We conducted one Friedman test for each response variable to determine if significant differences between analysis intervals existed. In order to counteract the problem of multiple comparisons by conducting one Friedman test per dependent variable, we used the Holm-Bonferroni correction and multiplied the p values by the respective correction factor [8]. This way, we can compare the corrected p values against the original significance level of $\alpha = 0.05$. The p values of all Friedman tests were lower than the significance level, thus allowing post-hoc tests for each dependent variable. As a post-hoc test, we applied the Wilcoxon test for paired data. We carried out post-hoc tests between Baseline_3, AfterCPT and HighestSBP[3]. We tested each of these intervals against each other, thereby creating non-orthogonal contrasts. Thus, we used the Holm-Bonferroni correction to adjust the p values of our post-hoc tests with the respective correction factor $(k-i+1)$ (with k being the number of conducted tests and i the rank of the p values sorted in ascending order). For vi-

[1] This situation occurs mostly due to immersion of the hand into the water and heavily affects the ROI. An altered ROI is likely to impact the results. As in [31], we excluded subjects who showed a high ROI variation in at least one of the considered analysis. The minimum correlation between a pair of ROI masks was set to 0.5.

[2] Note that the sum of subjects excluded due to each criterion exceeds the total number of excluded subjects. This is due to the fact that several subjects met more than one exclusion criterion. For all such criteria it holds, that if one analysis interval was affected, we excluded the whole participant.

[3] Baseline_1 and Baseline_2 were excluded from statistical testing because we did not expect a structural difference compared to Baseline_3, which is more closely related to the CPT.

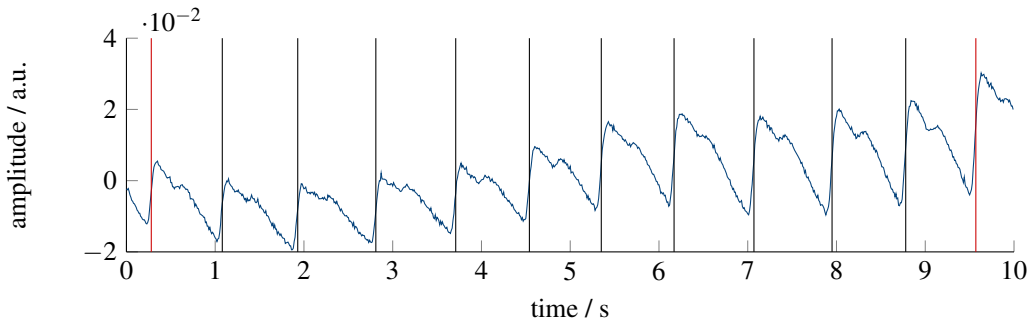

(a) Raw reference PPG signal

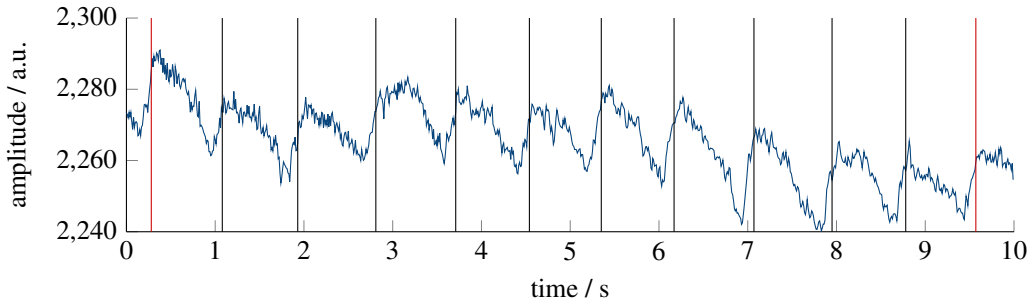

(b) Raw iPPG signal

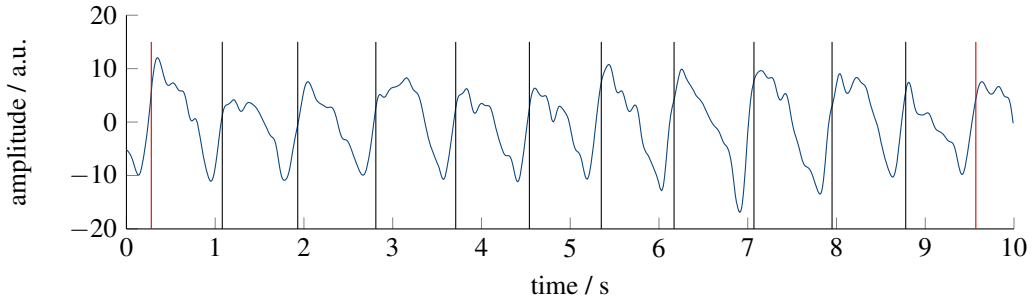

(c) Filtered iPPG signal

Figure 3: Exemplary illustration of PPG/iPPG signals from a single analysis interval. The vertical lines indicate the detected beats (detection took place in the reference PPG). Red lines indicate a detection which was not used for template generation. See figure 2 for an example on the template generation based on the filtered iPPG signal.

sualization purposes, we normalized all response variables to the mean of the three baseline measurements for the respective response variable. *I.e.*, all measures are given in arbitrary units, the baselines should be around 1 and values below 1 indicate a decrease whereas values over 1 indicate an increase.

3. Results

Figure 4 and figure 5 provide two examples for the template generation. While figure 4 shows rather homogeneous beat segments, figure 5 features a higher variability within the analysis intervals.

Figure 6a depicts ensembleAC of the iPPG data. ensembleAC shows a significant difference between AfterCPT and HighestSBP ($p < 0.01$). Apparently, ensembleAC drops at AfterCPT but quickly recovers and even slightly exceeds the baseline level during HighestSBP.

Figure 6b depicts ensembleAC of the reference PPG data. ensembleAC exhibits highly significant differences between Baseline_3 and AfterCPT ($p < 0.001$) as well as between Baseline_3 and HighestSBP ($p < 0.001$). According to that, the stimulus leads to a marked and persistent decrease of ensembleAC.

Figure 7 depicts the behaviour of the beat-to-beat intervals. The median reaches its minimum at AfterCPT. The median of HighestSBP is slightly below baseline level, but the values show a higher interquartile range. The length

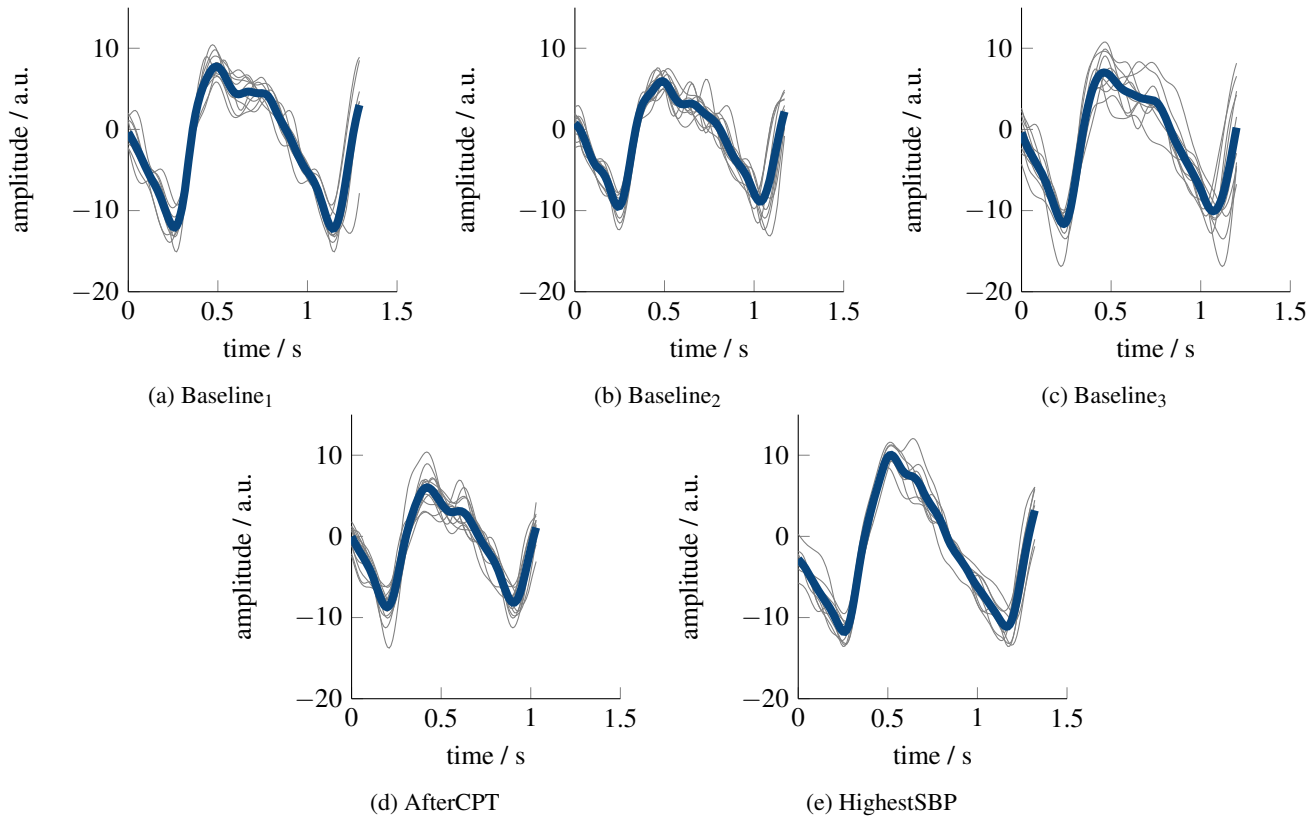

(a) Baseline$_1$ (b) Baseline$_2$ (c) Baseline$_3$

(d) AfterCPT (e) HighestSBP

Figure 4: Template generation for all analysis intervals of subject 4. Single beat segments are shown in light gray. The resulting template is shown in bold dark blue.

of the beat-to-beat intervals at AfterCPT was significantly different from both Baseline$_3$ ($p < 0.01$) and HighestSBP ($p < 0.05$).

4. Discussion

4.1. Explanation of the observed behaviour

We assume the CPT to cause pain thus triggering a sympathetic activation. The increase in sympathetic tone causes vasoconstriction in cutaneous vessels. [21, 23]

Our results show a decrease in ensembleAC and BBI during the immersion. Interestingly, the iPPG signals and the finger PPG signals show different reactions. Right after immersion, both signals exhibit a decrease. In the PPG signal this decrease is highly significant ($p < 0.01$). In the iPPG signal the decrease is not significant. However, a clearly decreasing trend can be observed visually. Past AfterCPT, the iPPG signal quickly recovers to values even slightly higher as at Baseline$_3$ while the finger PPG signal remains decreased.

A decrease in AC of the finger PPG is in accordance to the results of similar trials in literature [2, 7, 12, 20]. Awad *et al.* [2] and Jaryal *et al.* [12] explain this behaviour by a sympathetic activation. The activation causes an increased cardiac output and a marked vasoconstriction. The latter results in a decreased amplitude of the finger PPG. The sympathetic activation is also expected to increase the heart rate which is found in our data as well.

There are a few possible explanations for the distinct behaviour of iPPG and PPG signals. An obvious difference between the iPPG and PPG recordings are the respective measurement sites. Awad *et al.* [2] also report differences when comparing PPG signals obtained from the finger and the earlobe. They state the fingers' sympathetic responsiveness to be more pronounced than the earlobes' sympathetic responsiveness. The work of Budidha and Kyriacou [5] supports these findings. In fact, not only the sympathetic responsiveness of the finger but of the extremities in general is very high [21], eventually also higher than the sympathetic responsiveness of the head and forehead. The systemic blood pressure increase, thus, is predominantly driven by vasoconstriction in the extremities. Facial vasoconstriction is comparatively less pronounced. The initial drop in iPPG's AC might express slight local vasoconstriction. The increased cardiac output and blood pressure, note that with

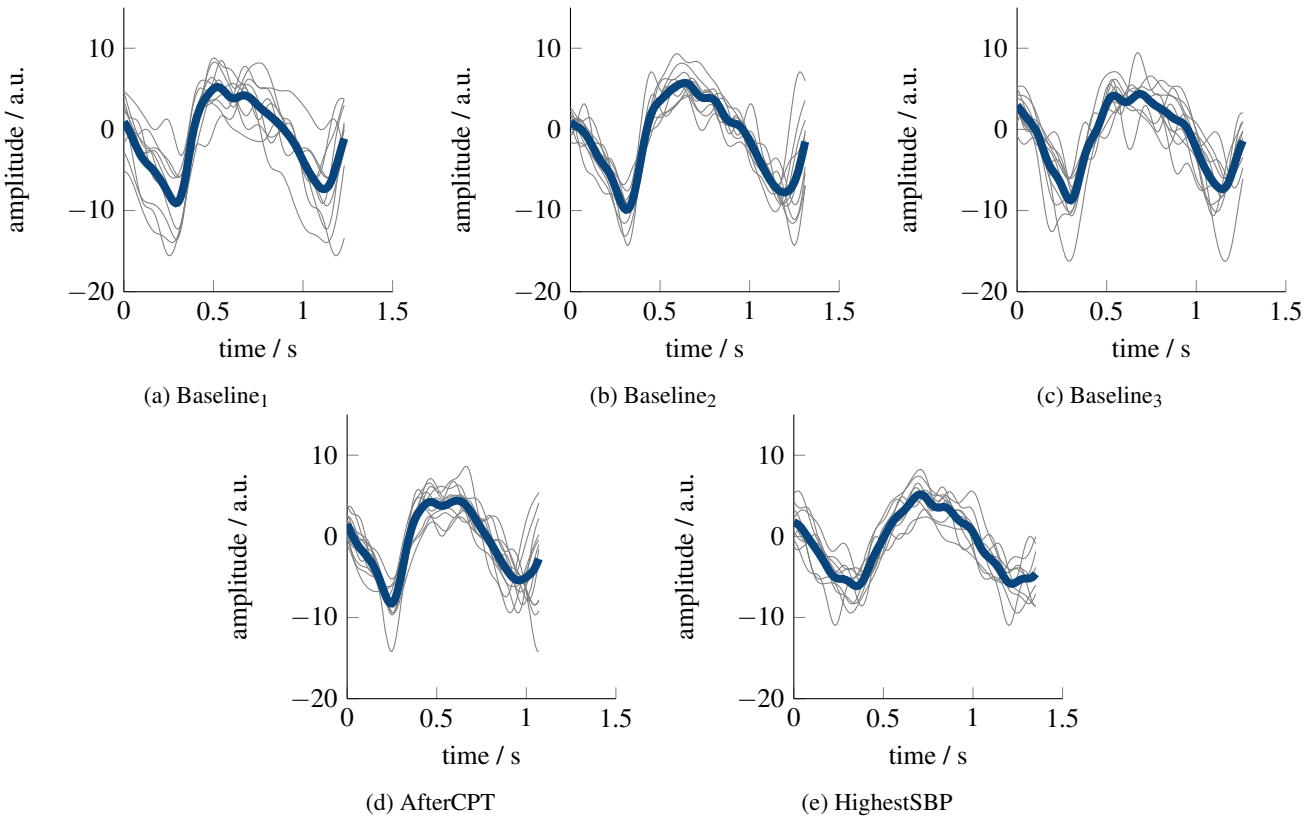

(a) Baseline$_1$ (b) Baseline$_2$ (c) Baseline$_3$

(d) AfterCPT (e) HighestSBP

Figure 5: Template generation for all analysis intervals of subject 5. Single beat segments are shown in light gray. The resulting template is shown in bold dark blue. In comparison to figure 4, the individual beats of this subject show a much more pronounced variability.

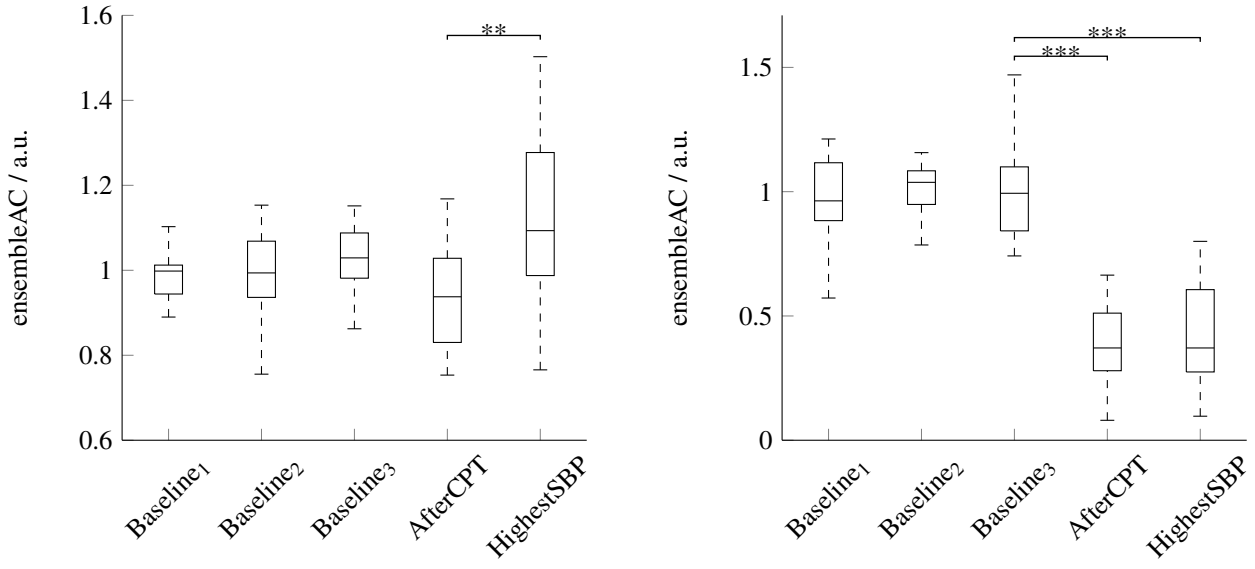

(a) Green channel of the camera recordings (b) Reference PPG

Figure 6: Results for the analysis of ensembleAC over all analysis intervals, depicted by boxplots. If significant, post-hoc tests' outcome is denoted by * $p < 0.05$, ** $p < 0.01$ or *** $p < 0.001$. Outliers are not shown.

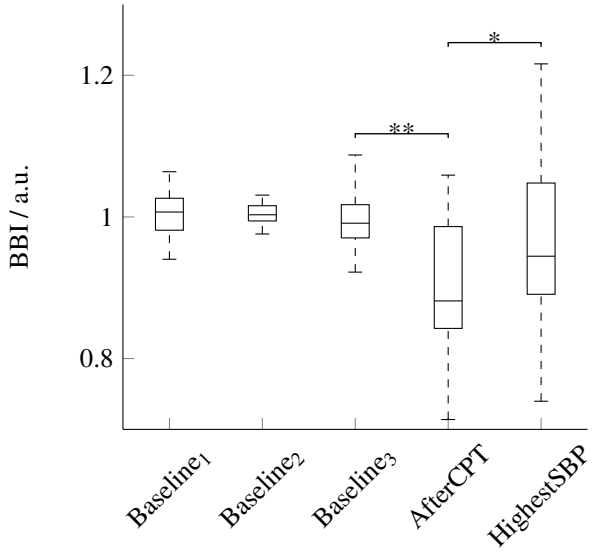

Figure 7: Results for the analysis of the beat-to-beat intervals over all analysis intervals, depicted by boxplots. If significant, post-hoc tests' outcome is denoted by * $p < 0.05$, ** $p < 0.01$ or *** $p < 0.001$. Outliers are not shown.

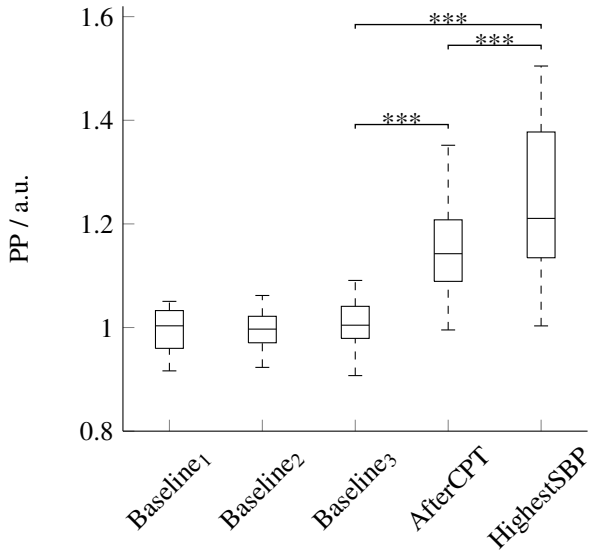

Figure 8: Results for the analysis of the pulse pressure over all analysis intervals, depicted by boxplots. If significant, post-hoc tests' outcome is denoted by * $p < 0.05$, ** $p < 0.01$ or *** $p < 0.001$. Outliers are not shown.

increased SBP also the pulse pressure increases (see figure 8), afterwards leads to a more pronounced pulsation, *i.e*. an inverse effect in iPPG as one could expect from finger PPG.

One could also assume that the used color channel has an impact on the differing results. In fact, the reference PPG signal is derived from an infrared photoelectric sensor while we use the green channel of the video recordings for iPPG. In order to rule out the difference in wavelengths as an explanation, we examined the recordings of the NIR camera. In comparison to the green channel, the NIR channel exhibits a poor signal-to-noise ratio (see figure 9). As a result, in many cases no reliable beat templates could be established. As described before, this would lead to an exclusion of the respective analysis interval and thus of the whole participant. We therefore decided to include the NIR recordings only for qualitative visual analyses. Figure 10 shows the AC for all segments which could be derived. The results do not resemble the behaviour of the finger PPG but rather the green channel. Therefore, we do not consider the different wavelengths to be the reason for our findings.

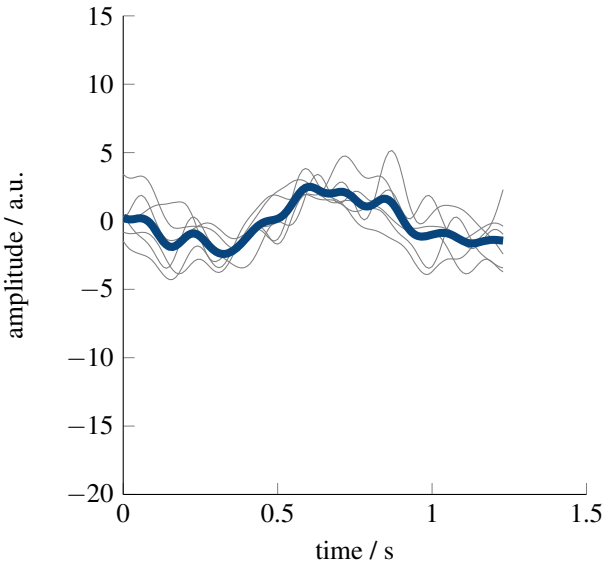

Figure 9: Exemplary template generation for the NIR channel of the same subject and epoch as in figure 2. Single beat segments are shown in light gray. The resulting template is shown in bold dark blue.

A third possible explanation stresses the origin of the iPPG and PPG signal. The origin and contributing factors of the iPPG signal have been debated in literature [13, 18, 32]. Compared to the finger PPG, the iPPG penetrates less into the skin. iPPG signals are thus generally, *i.e*. independently of the used wavelength, likely to be more affected by superficial vessels whereas the conventional PPG also captures deeper vessels. As a consequence, iPPG may not be heavily influenced by vessels that show vasoconstriction by themselves. It thus reflects the microcirculation whereas conventional PPG rather reflects the macrocirculation. As a result, sympathetic activation damps the pulsation upstream to the iPPG-relevant vessels, which leads to a short drop in iPPG's AC. The increase in blood pressure then compensates for this damping leading to similar pulsation in iPPG-relevant

vessels compared to the pre-stimulus state.

To summarize, we cannot explain the disparity in behaviour of the PPG and iPPG signals with certainty. It is also likely that different factors contribute to our finding. However, our results are in line with previous findings that showed a strong correlation between the iPPG signal's AC and the systemic pulse pressure [26]. Moreover, the observation itself has relevance for the interpretation of iPPG signals and and the design of future use cases of the technique beyond remote heart rate assessment. In particular, care should be taken when expectations on finger PPG are to be transferred to iPPG or finger PPG is used as ground truth in studies beyond heart rate assessment.

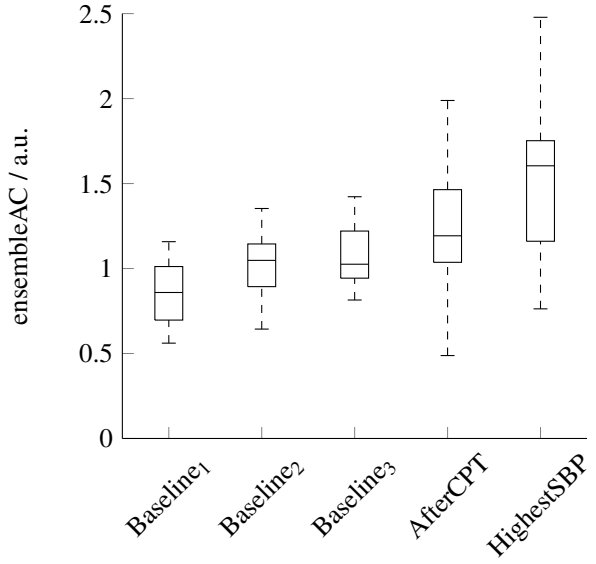

Figure 10: Results for the analysis of ensembleAC from the NIR channel of the camera recordings over all analysis intervals, depicted by boxplots. The exclusion criteria were not applied to the values used to create this figure. Outliers are not shown.

4.2. Limitations

The presented work has some limitations. Generally, the required exclusion criteria lead to a rather small population, which shows a relatively high variability. Results of such analysis should be taken with care. Within the analysis, the determination of analysis intervals is troublesome. Actually different person show different types of reaction and exhibit different time courses in their reaction. Against that background, it is not easy to define intervals that are inter-individually comparable.

5. Outlook

As we cannot fully explain the disparity in behaviour of the PPG and iPPG signals, future works should address this issue. Therefore, it will be necessary to further investigate the origin of the iPPG signal. Also, the morphology of the iPPG signal could be examined by more complex methods like pulse wave decomposition as these methods have proven to reveal valuable information about the cardiovascular system.

Acknowledgements

This work was funded by the Deutsche Forschungsgemeinschaft (DFG, German Research Foundation) - 401786308.

References

[1] J. Allen. Photoplethysmography and its application in clinical. *Physiological Measurement*, 28(3):1 – 39, 2007.

[2] A. A. Awad, M. A. M. Ghobashy, W. Ouda, R. G. Stout, D. G. Silverman, and K. H. Shelley. Different responses of ear and finger pulse oximeter wave form to cold pressor test. *Anesthesia and Analgesia*, 92(6):1483–1486, 2001.

[3] H. J. Baek, J. S. Kim, Y. S. Kim, H. B. Lee, and K. S. Park. Second Derivative of Photoplethysmography for Estimating Vascular Aging. In *2007 6th International Special Topic Conference on Information Technology Applications in Biomedicine*, volume 893, pages 70–72. IEEE, nov 2007.

[4] L. A. Bortolotto, J. Blacher, T. Kondo, K. Takazawa, and M. E. Safar. Assessment of vascular aging and atherosclerosis in hypertensive subjects: Second derivative of photoplethysmogram versus pulse wave velocity. *American Journal of Hypertension*, 13(2):165–171, 2000.

[5] K. Budidha and P. A. Kyriacou. Photoplethysmography for quantitative assessment of sympathetic nerve activity (SNA) during cold stress. *Frontiers in Physiology*, 10(JAN):1–10, 2019.

[6] K. Chellappan, M. A. Mohd Ali, and E. Zahedi. An Age Index for Vascular System Based on Photoplethysmogram Pulse Contour Analysis. In *4th Kuala Lumpur International Conference on Biomedical Engineering 2008*, volume 21, pages 125–128. Springer Berlin Heidelberg, Berlin, Heidelberg, 2008.

[7] K. Hamunen, V. Kontinen, E. Hakala, P. Talke, M. Paloheimo, and E. Kalso. Effect of pain on autonomic nervous system indices derived from photoplethysmography in healthy volunteers. *British Journal of Anaesthesia*, 108(5):838–844, may 2012.

[8] S. Holm. A simple sequential rejective method procedure. *Scandinavian Journal of Statistics*, 6(2):65–70, 1979.

[9] B. D. Holton, K. Mannapperuma, P. J. Lesniewski, and J. C. Thomas. Signal recovery in imaging photoplethysmography. *Physiological Measurement*, 34(11):1499–1511, 2013.

[10] M. Huelsbusch and V. Blazek. Contactless mapping of rhythmical phenomena in tissue perfusion using PPGI. In *Proc.*

SPIE 4683, Medical Imaging 2002: Physiology and Function from Multidimensional Images, number April 2002, pages 110 – 117, 2002.

[11] M. Huotari, A. Vehkaoja, K. Määttä, and J. Kostamovaara. Photoplethysmography and its detailed pulse waveform analysis for arterial stiffness. *Journal of Structural Mechanics*, 44(4):345–362, 2011.

[12] A. K. Jaryal, N. Selvaraj, J. Santhosh, S. Anand, and K. K. Deepak. Monitoring of Cardiovascular Reactivity to Cold Stress Using Digital Volume Pulse Characteristics in Health and Diabetes. *Journal of Clinical Monitoring and Computing*, 23(2):123–130, apr 2009.

[13] A. A. Kamshilin, E. Nippolainen, I. S. Sidorov, P. V. Vasilev, N. P. Erofeev, N. P. Podolian, and R. V. Romashko. A new look at the essence of the imaging photoplethysmography. *Scientific Reports*, pages 1–9, 2015.

[14] A. A. Kamshilin, V. V. Zaytsev, and O. V. Mamontov. Novel contactless approach for assessment of venous occlusion plethysmography by video recordings at the green illumination. *Scientific Reports*, 7(1):1–9, 2017.

[15] J. Lazaro, E. Gil, J. M. Vergara, and P. Laguna. Pulse Rate Variability Analysis for Discrimination of Sleep-Apnea-Related Decreases in the Amplitude Fluctuations of Pulse Photoplethysmographic Signal in Children. *IEEE Journal of Biomedical and Health Informatics*, 18(1):240–246, 2014.

[16] H. E. Liu, Y. Wang, and L. E. I. Wang. The Effect of Light Conditions on Photoplethysmographic Image Acquisition Using a Commercial Camera. *IEEE Journal of Translational Engineering in Health and Medicine*, 2, 2014.

[17] E. A. López-Beltrán, P. L. Blackshear, S. M. Finkelstein, and J. N. Cohn. Non-invasive studies of peripheral vascular compliance using a non-occluding photoplethysmographic method. *Medical and Biological Engineering and Computing*, 36(6):748–753, 1998.

[18] A. V. Moço, S. Stuijk, and G. De Haan. New insights into the origin of remote PPG signals in visible light and infrared. *Scientific Reports*, 8(1):1–15, 2018.

[19] I. Nishidate, C. Tanabe, D. J. McDuff, K. Nakano, K. Niizeki, Y. Aizu, and H. Haneishi. RGB camera-based non-contact imaging of plethysmogram and spontaneous low-frequency oscillation in skin perfusion before and during psychological stress. In G. L. Coté, editor, *Optical Diagnostics and Sensing XIX: Toward Point-of-Care Diagnostics*, volume 1088507, page 7. SPIE, feb 2019.

[20] H. Njoum and P. A. Kyriacou. Investigation of finger reflectance photoplethysmography in volunteers undergoing a local sympathetic stimulation. *Journal of Physics: Conference Series*, 450(1), 2013.

[21] H.-C. Pape, A. Kurtz, and S. Silbernagl. *Physiologie*. Georg Thieme Verlag, 2018.

[22] M.-Z. Poh, D. J. McDuff, and R. W. Picard. Non-contact, automated cardiac pulse measurements using video imaging and blind source separation. *Optics Express*, 18(10):10762 – 10774, 2010.

[23] R. F. Schmidt, F. Lang, and M. Heckmann. *Physiologie des Menschen*. Springer, 10 edition, 2010.

[24] N. Skoluda, J. Strahler, W. Schlotz, L. Niederberger, S. Marques, S. Fischer, M. V. Thoma, C. Spoerri, U. Ehlert, and U. M. Nater. Intra-individual psychological and physiological responses to acute laboratory stressors of different intensity. *Psychoneuroendocrinology*, 51:227–236, jan 2015.

[25] K. Takazawa, N. Tanaka, M. Fujita, O. Matsuoka, T. Saiki, M. Aikawa, S. Tamura, and C. Ibukiyama. Assessment of Vasoactive Agents and Vascular Aging by the Second Derivative of Photoplethysmogram Waveform. *Hypertension*, 32(2):365–370, aug 1998.

[26] A. Trumpp, S. Rasche, D. Wedekind, M. Rudolf, H. Malberg, K. Matschke, and S. Zaunseder. Relation between pulse pressure and the pulsation strength in camera-based photoplethysmograms. *Current Directions in Biomedical Engineering*, 3(2):489–492, 2017.

[27] A. Trumpp, J. Schell, H. Malberg, and S. Zaunseder. Vasomotor assessment by camera-based photoplethysmography. *Current Directions in Biomedical Engineering*, 2(1):199–202, 2016.

[28] W. Verkruysse, L. O. Svaasand, and J. Nelson. Remote plethysmographic imaging using ambient light. *Optics Express*, 16(26):21434–21445, 2008.

[29] L. Wang, E. Pickwell-MacPherson, Y. Liang, and Y. Zhang. Noninvasive cardiac output estimation using a novel photoplethysmogram index. In *2009 Annual International Conference of the IEEE Engineering in Medicine and Biology Society*, pages 1746–1749. IEEE, sep 2009.

[30] W. Wang, A. C. Den Brinker, S. Stuijk, and G. De Haan. Robust heart rate from fitness videos. *Physiological Measurement*, 38(6):1023–1044, 2017.

[31] S. Zaunseder, A. Trumpp, H. Ernst, M. Förster, and H. Malberg. Spatio-temporal analysis of blood perfusion by imaging photoplethysmography. *Optical Diagnostics and Sensing XVIII: Toward Point-of-Care Diagnostics*, 10501(February):15, 2018.

[32] S. Zaunseder, A. Trumpp, D. Wedekind, and H. Malberg. Cardiovascular assessment by imaging photoplethysmography – a review. *Biomedical Engineering/Biomedizinische Technik*, pages 1–18, 2018.